Decarbonizing Industrial Heat in Central Asia: A Case Study on Parabolic Trough Collectors under Tashkent Conditions

Azizboy Khaitmukhamedov, Dilshod Jalilov and Oybek Abdulkhaev

Physical-Technical Institute of Uzbekistan Academy of Sciences, Tashkent (Uzbekistan)

Abstract

Decarbonizing industrial process heat is critical for meeting global climate targets, yet developing economies heavily reliant on fossil fuels face severe barriers, including economic constraints and catastrophic wintertime air pollution. Here, we present a comprehensive techno-economic and environmental optimization of parabolic trough collector (PTC) systems for solar heat for industrial processes (SHIP), using the highly polluted, fossil-dependent urban airshed of Tashkent as a representative model. By simulating scenarios across varying capacities (5–20 MW_{th}) and temperatures (60–390 °C), we identify critical design thresholds for the solar multiple and thermal energy storage. We show that optimized low-to-mid-temperature configurations achieve a ~46% capacity factor with a levelized cost of heat of ~3.6 ¢/kWh_{th}, while high-temperature setups optimize at a ~41% capacity factor with a cost of ~4.0 ¢/kWh_{th}, both successfully outperforming current European benchmarks. System robustness is verified through comprehensive multi-factor sensitivity analyses encompassing both meteorological attenuation and macroeconomic shocks. Furthermore, we quantify the substantial reductions in CO_2, NO_x, SO_2, and $PM_{2.5}$ emissions achievable by displacing fossil-fueled boilers during peak smog seasons. Our findings demonstrate that appropriately sized PTC-SHIP systems are not only technically feasible but economically highly competitive in emerging markets. This provides a replicable, cost-effective pathway for policymakers to simultaneously decarbonize industrial heat and drastically improve urban public health in the Global South.

Keywords: Parabolic trough collector, levelized cost of heat, System Advisor Model, industrial heat, thermal energy output

1. Introduction

Fossil fuel reliance remains a major driver of greenhouse gas emissions and is accelerating climate change. Improving energy efficiency is increasingly seen as crucial for mitigation and a transition to sustainable energy. Fossil fuel use also leads to air pollution, resource depletion, and climate disruptions, underscoring an urgent need for cleaner renewable energy sources. Solar thermal technologies offer a promising solution, providing heat for industrial processes without harmful emissions. Industries worldwide are increasingly adopting renewable heat sources such as solar energy to comply with environmental regulations and stabilize energy costs, as reported by REN21 (2023). For instance, in 2020 over 40% of energy-related CO_2 emissions came from industrial heat (mostly fossil-fueled), while renewables provided under one-quarter of industrial energy. Decarbonizing heat supply is thus a priority, and technologies like concentrated solar power (CSP) can significantly reduce industrial emissions. CSP costs have fallen by about 68% since 2010, making these systems increasingly competitive. Consequently, CSP's share in the global energy mix is expected to increase substantially by 2050, thereby contributing to the transition toward a low-carbon economy, according to El Ydrissi et al. (2020).

Among CSP options for heat, parabolic trough collector (PTC) systems are especially effective. Industrial facilities can choose from various solar collectors: flat-plate and evacuated tube collectors suffice for low-temperature needs (up to ~100 °C), whereas concentrating collectors like linear Fresnel and PTC can reach ~400 °C. PTC technology is highly efficient in the mid-temperature range (~80–250 °C), which covers many process heat applications (e.g., steam generation, drying). Reflecting this potential, solar heat for industrial processes (SHIP) has seen increasing adoption worldwide. By 2020, approximately 891 SHIP systems, with a total collector area exceeding 1 million m², were in operation, primarily in sunny countries such as Mexico, India, and the USA, according to Weiss et al. (2024). This growth continued through 2022, with more than

10.18086/swc.2025.01.06 Available at http://proceedings.ises.org

1000 SHIP installations, representing a cumulative capacity of over 856 MW_{th}, supplying clean heat to a wide range of industries, according to REN21 (2023). Flat-plate collectors account for most installations, but PTC-based systems are the second most common-underscoring their popularity for medium-temperature industrial heating. Importantly, CSP for heat has demonstrated strong practical potential, particularly in water purification and water heating applications, and is often more cost-effective for thermal energy generation than for electricity production, according to Kumar et al. (2019). These developments show that solar thermal solutions like PTC are both technically viable and economically attractive for industrial heat supply.

Despite global progress, local challenges underscore the need to shift away from fossil-fueled heating. In Tashkent, Uzbekistan's capital, heavy reliance on fossil fuel for heat has led to severe air pollution. Wintertime fine particulate ($PM_{2.5}$) levels are alarmingly high, reaching up to 15 times the recommended limit during severe smog episodes. On an annual basis, $PM_{2.5}$ averages above 30 μg/m³-over six times the WHO guideline of 5 μg/m³-contributing to an estimated 3000 premature deaths each year. The problem is most acute in winter, when heating demand peaks (Fig. 1).

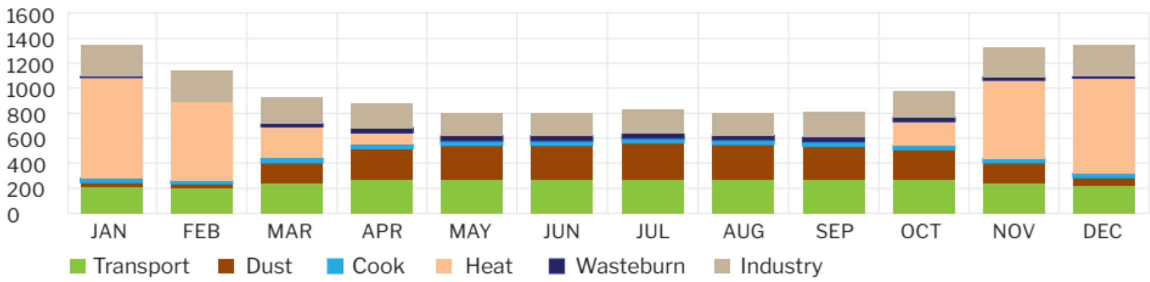

Figure 1: Monthly variation in $PM_{2.5}$ emissions in Tashkent, adapted from the World Bank (2024).

Tashkent's emissions show strong seasonal variation driven by temperature-dependent energy use. As shown in Fig. 1, space heating contributes up to ~60% of monthly $PM_{2.5}$ in winter but is negligible in summer. Emissions from transportation stay relatively constant year-round, urban dust peaks in summer due to construction and resuspended particles, and industrial sources emit at a steady baseline throughout the year. These patterns underscore the urgent need for seasonally adaptive, sustainable heat supply systems. Solar thermal technologies-especially PTCs-can play a vital role in reducing winter emissions by replacing a portion of fossil-fueled heating. Because peak pollution coincides with peak heating demand, solar-assisted heating can directly cut harmful air pollutants while advancing decarbonization goals.

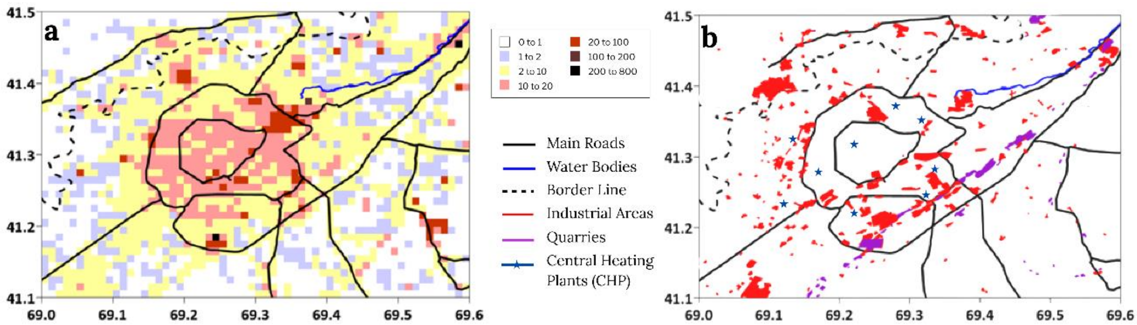

Figure 2: Annual average PM2.5 emissions map (a) and industrial areas (b) in the Tashkent airshed, 2021 (tons per grid-year).

Coal-based heating is the single largest contributor to Tashkent's winter $PM_{2.5}$ pollution. Recent assessments attribute nearly 45% of $PM_{2.5}$ in peak winter months to coal combustion for heat. A significant share of these emissions originates in peri-urban areas surrounding the city, but it still strongly affects urban air quality through atmospheric transport, according to the World Bank (2024). Fig. 2a highlights several emission hotspots across the Tashkent airshed. Particularly high concentrations occur in the northeastern part of the city (near the second ring road) and in the southern Yangikhayot district-an area of dense industrial activity (Fig. 2b). Tashkent's industrial facilities can be categorized into heavy industry (e.g., a thermal power plant, metal processing plant, foundry) versus light industry (smaller manufacturing sites). Fig. 2b also marks nine central heating plants (CHPs) that supply district heating across the city, some of which serve nearby industry. These CHPs are crucial for winter heating but, because they burn fossil fuels, significantly contribute to local air pollution. Overall, fossil-fueled heating clearly drives Tashkent's air pollution problem, and cutting emissions from this sector is an urgent public health priority.

Reducing pollution in Tashkent requires replacing coal- and gas-based heating with cleaner alternatives. Uzbekistan's heat supply is still dominated by fossil fuels, with natural gas alone providing about 85% of industrial energy use, driving air pollution, greenhouse gas emissions, and fuel price vulnerability. Yet this dependence also creates a major opportunity: even partial substitution of renewable heat can bring clear environmental and economic gains. PTC-based solar thermal systems can nearly eliminate on-site emissions and reduce operating costs by using free solar energy. This is especially relevant amid rising gas prices and government incentives for green investment in Uzbekistan. A transition to renewable heating would improve urban air quality while strengthening energy and economic security.

Uzbekistan has set ambitious energy transition targets for 2030, including adding about 19 GW of renewable capacity, raising the renewable share in power generation to around 54%, and reducing greenhouse gas emissions by at least 35%. Achieving these goals will require major reforms in the energy and heating sectors, especially in urban areas such as Tashkent. At the same time, the country has strong solar potential, with many regions receiving up to ~3200 sunshine hours and 1800–2000 kWh/m² of annual solar irradiation, according to Avezova et al. (2018). Using this resource for heating could reduce fossil fuel dependence, improve air quality, and support decarbonization goals.

PTC technology emerges as a sustainable solution for Tashkent's heating dilemma. PTC-based solar thermal systems can replace or supplement traditional coal and gas boilers, providing required heat for industrial processes or district heating without harmful emissions. The environmental benefits are twofold: a reduction in greenhouse gas emissions and a near-elimination of localized air pollutants. Indeed, the use of PTC systems for heat generation can substantially reduce CO_2 and criteria pollutant emissions (NO_x, SO_2, and PM) compared with fossil-fuel-based sources, according to Mohammadi et al. (2021). Solar heat produces no on-site combustion emissions, improving urban air quality and mitigating health risks. Moreover, modern PTC systems can achieve the temperature ranges needed for most industrial and residential heating applications, so switching to solar heat does not compromise performance. Ongoing technological advances, including improved mirror optics and tracking systems reported by Wu et al. (2022), enhanced heat transfer fluids (including nanofluids), and better thermal storage integration, continue to improve the efficiency and cost-effectiveness of PTC installations, as highlighted by Jalilov et al. (2024). These innovations are driving down the levelized cost of heat and making solar thermal projects increasingly attractive to investors and policymakers. Thus, from both environmental and techno-economic perspectives, PTC offers a viable pathway to curb Tashkent's air pollution while supporting Uzbekistan's sustainable energy trajectory.

Motivated by this context, this study evaluates the technical, economic, and environmental performance of PTC systems for solar process heat under Tashkent's climate. Four representative SHIP scenarios, covering capacity of about 10 MW_{th} and process temperatures from ~60–120 °C to ~290–390 °C, were modeled in NREL's SAM using local weather data. Key parameters, including solar multiple and thermal energy storage capacity, were optimized to minimize the levelized cost of heat (LCOH). The analysis includes annual energy yield, economic performance, and avoided emissions, allowing identification of the most suitable PTC configuration for local conditions. Overall, the results demonstrate the potential of solar thermal systems to support cleaner and more cost-effective industrial heating in Uzbekistan.

2. Methodology

In this study, the System Advisor Model (SAM) was used to simulate the impact of key design parameters – notably the solar multiple (SM) and thermal energy storage (TES) capacity – on PTC-based SHIP configurations, in order to identify optimal designs. The simulations examine how varying these parameters affects annual energy production and the resulting levelized cost of heat (LCOH). SAM performs detailed hourly performance and financial modeling of the system, as described by Jain et al. (2013), and enables parametric analyses to assess how changes in design, cost, and financial inputs affect the results, according to NREL (2023).

SAM was configured with Tashkent's typical meteorological year (TMY) climate data, including hourly direct normal irradiance (DNI) values, following Shirmohammadi et al. (2021). Because PTC performance depends primarily on direct solar radiation, accurate DNI data are essential, as noted by Mukeshimana et al. (2021). For Tashkent, the total annual DNI is about 1653 kWh/m² (Fig. 3), which falls within the favorable range of 1600-2000 kWh/m² considered suitable for viable PTC projects, according to Wang (2019). This indicates that Tashkent has sufficient solar resource (strong summer sun, limited winter sun) for effective PTC operation.

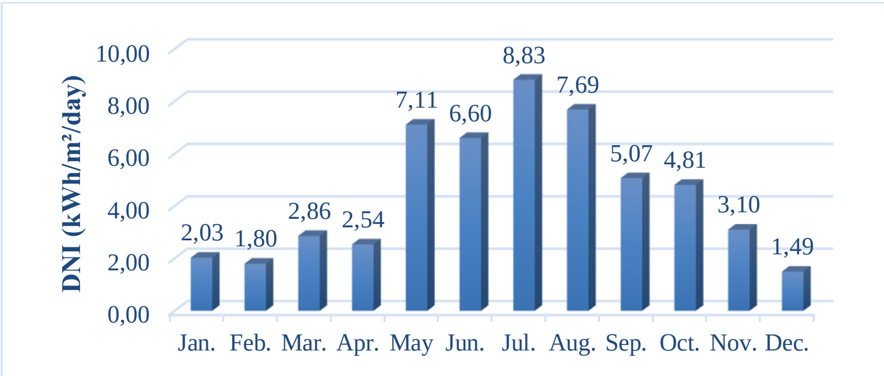

Figure 3: Average monthly DNI (kWh/m²/day) for Tashkent.

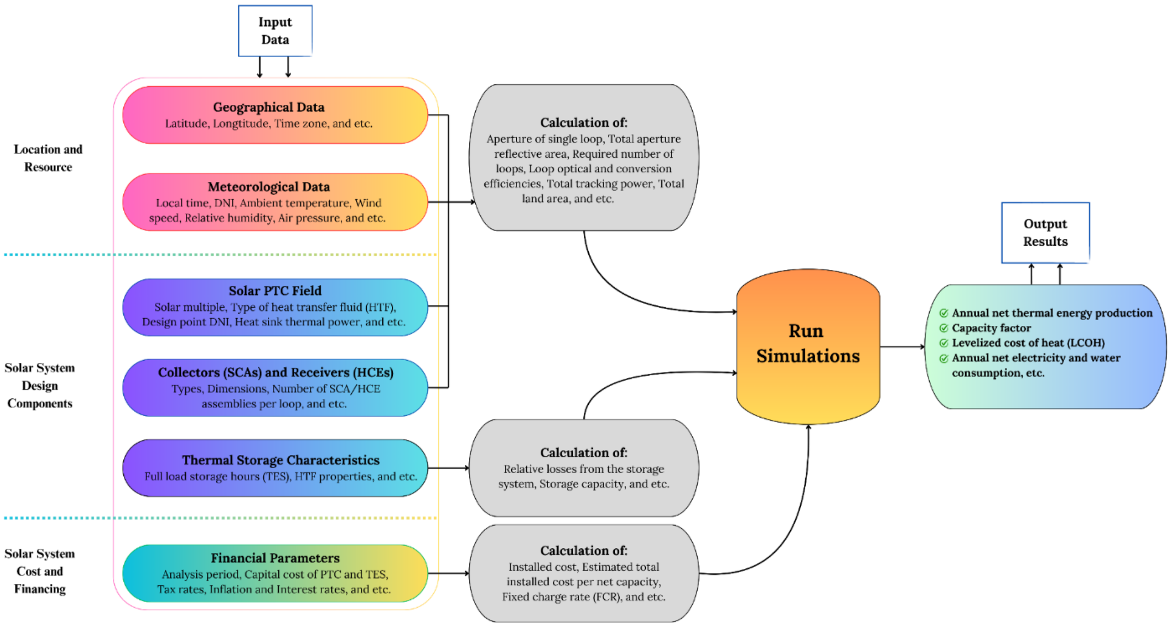

Figure 4: Block diagram of the solar PTC system simulated using SAM software, adapted from Akello et al. (2023).

The system model was developed based on the schematic shown in Fig. 4, which was adapted from Akello et al. (2023), which illustrates the relationships between the solar field components. We analyzed four representative PTC scenarios covering low (~60–120 °C), medium (~100–250 °C), and high (~290–390 °C) process heat requirements, based on the classification reported by Lovegrove et al. (2020). In each case, the heat transfer fluid (HTF) outlet temperature was set approximately 15 °C above the required process temperature to account for thermal losses between the solar field and the end-use process, following Manikandan et al. (2019). Every case assumed a 10 MW_{th} heat sink (thermal demand). In all cases, the same PTC collector technology (FLABEG Ultimate Trough RP6 with Schott PTR80 receivers) and heat transfer fluid (HTF; Therminol VP-1) were used, following Steinfeld et al. (2014).

In each simulation, the solar multiple was varied from 1 to 3. The solar multiple is a key design parameter, defined as the ratio of the solar field's thermal output under design conditions to the plant's thermal demand under nominal conditions, following Montes et al. (2009). A larger SM corresponds to a larger collector field (more reflective area), enabling the system to generate more thermal energy.

TES plays a crucial role by storing excess solar heat for use during periods when solar radiation is insufficient. A parametric analysis was carried out to evaluate various combinations of SM and TES capacity, revealing the performance benefits and trade-offs of different configurations. Incorporating TES to buffer the heat supply as needed increases the system's overall energy efficiency. In our model, the HTF itself (Therminol VP-1) is used as the storage medium in a single-tank design, which simplifies the system and reduces cost. All other secondary inputs (efficiencies, losses, etc.) were left at SAM's default settings.

Financial parameters and system cost assessment. We then used SAM's financial model to evaluate the economics of each PTC-SHIP configuration, focusing on the LCOH (the total cost of thermal energy over the system's lifetime). The economic analysis accounts for the initial capital investment and the annual operating expenses (including operation and maintenance). Important financial metrics in the model include the Fixed Charge Rate (FCR), which incorporates factors like the capital recovery and project financing costs, and the weighted average cost of capital (WACC), which represents the cost of funding the project (blending debt and equity) adjusted for taxes.

For the financial evaluation, a project lifetime of 25 years was assumed. Key macroeconomic parameters for Uzbekistan were set as follows: an inflation rate of 10.5% and an annual interest rate of 13.5%, according to the Central Bank of Uzbekistan (2025); a value-added tax (VAT) of 12%; and a profit tax of 15% as indicated by the Tax Committee (2025). The target internal rate of return (IRR) for the project is 15%, which aligns with the recommended values for similar investments reported by Aly et al. (2019). These inputs establish the project's financial framework for viability assessment.

Based on cost modeling, the solar field was estimated to cost around \$204 per m^2, as used by Dersch et al. (2020), and the TES cost was derived using SAM's thermal storage sizing model, following the approach of Glatzmaier's (2011). (For reference, Tab. 1 lists the unit cost assumptions for major components such as the solar field, TES, and other subsystems.) After specifying these cost parameters, all remaining financial inputs used SAM's default values to ensure consistency.

Table 1: Costs for installation used by Dersch et al. (2020) and Glatzmaier (2011).

Parameters	Value
Site improvements	25 \$/m^2
Solar field	127 \$/m^2
HTF system	52 \$/m^2
Storage	40 \$/$kW{\cdot}h_{th}$
Heat sink	120 \$/kW_{th}
Balance of plant	90 \$/kW_{th}

3. Results and Discussion

In this section, the results obtained using the SAM, described in the methodology section and applied to typical cases of SHIP, are discussed. The analysis of parameters such as the solar multiple (SM, ranging from 1 to 3) and the duration of the thermal energy storage system operation (TES, from 0 to 15 hours), allowed for the assessment of the efficiency of various SHIP system configurations. The simulation results demonstrate how changes in SM and TES affect the annual amount of thermal energy produced, the level of LCOH, and the capacity factor (CF).

Optimizing SHIP plants requires selecting the TES capacity and solar field size (SM) to minimize the overall LCOH while maintaining the required capacity factor (CF). In this study, the optimal design was defined as the point at which further increases in TES or SM reduced LCOH by less than 1% for PTC systems. This criterion was chosen because, at the pre-commercial assessment stage, small additional LCOH reductions do not justify the significantly higher capital costs and financial risks. In practice, SHIP developers therefore seek not only the minimum LCOH, but also a balanced trade-off between cost reduction, capital investment, and reliable CF.

The following presents key results from the simulation of SHIP installations, including analysis of optimized projects. The main economic and technical indicators include the LCOH, the annual amount of thermal energy produced, and the CF, which reflects the ratio of actual energy generated to the theoretically possible energy when the system operates at full capacity.

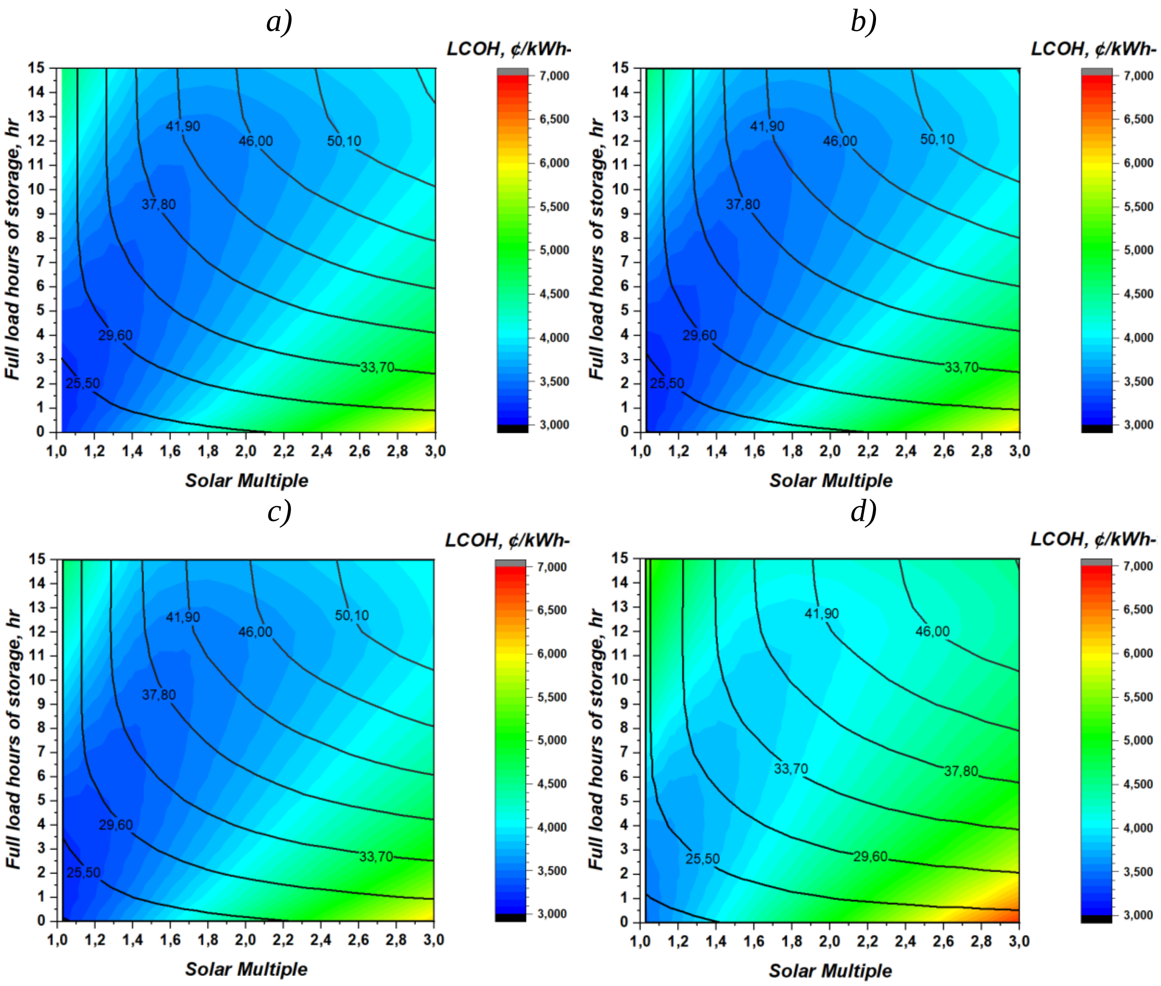

Figure 5: The impact of the TES system duration and SM size on the LCOH and the CF for various cases, considering a heat sink with a thermal capacity of 10 MW_{th}. a) Case 1; b) Case 2; c) Case 3; d) Case 4. In the graphs, LCOH is represented as a color gradient, while CF is depicted using contours.

Fig. 5 demonstrates the impact of operation of the TES system duration and the size of the SM on LCOH and the CF of various configurations of solar thermal plants with heat sink thermal capacity of 10 MW_{th}. In the charts, LCOH is represented by a color gradient, while CF is visualized as contours. The data analysis shows that both LCOH and CF increase with the growth of the SM and the duration of TES operation. However, the relationships between these indicators differ and exhibit somewhat opposite characteristics.

Unlike the CF, the dependency of LCOH on the size of the SM and the capacity of the TES system manifests differently. An excessively large solar field with small TES capacities leads to significant thermal energy losses, since the heat sink cannot utilize all the thermal energy generated by the solar field over many hours. A high SM allows the installation to operate under design conditions for most of the year but requires the dumping of excess solar energy during a significant part of the summer. Without energy storage, installations relying solely on solar energy are limited to annual CF around 25%, as shown in Fig. 5.

On the other hand, with low SM values and an excessively large TES system, another problem arises: the solar field fails to provide enough additional thermal energy to meet the high demand of the heat sink. As a result, the significant increase in net capital costs due to a large TES system is not compensated by the increase in useful thermal energy production.

The heat sink capacity has minimal impact on LCOH and CF, except in cases with a solar thermal plant based on PTC. Here, where the inlet and outlet temperatures of the HTF are 290°C and 390°C respectively, the impact of the heat sink capacity becomes more pronounced.

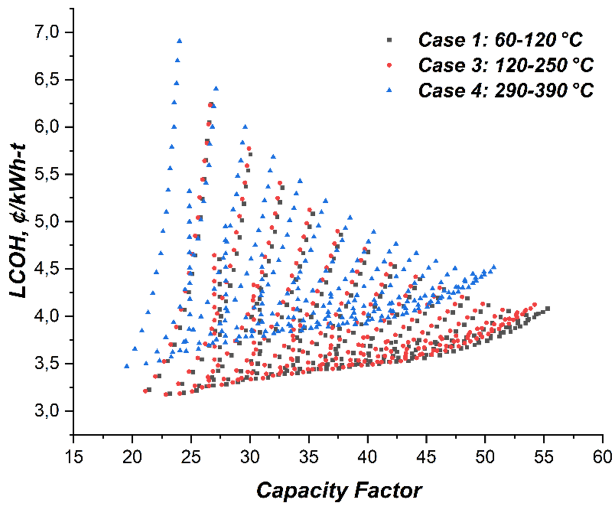

Figure 6: LCOH, in ¢/kWh$_{th}$ versus CF, in % for PTC thermal systems providing a 10 MW$_{th}$ industrial heat load in Tashkent, for three process temperature ranges: Case 1, Case 3, and Case 4. Each data point is a SAM simulation result for a specific system configuration (varying SM and TES capacity), illustrating how design choices that raise CF (larger collector fields and added storage) affect the delivered heat cost in each temperature scenario.

The representation of the LCOH with a color gradient and the CF in the form of contours allows for the determination of the capacity values for TES and SM that enable the achievement of an optimal project with the lowest LCOH at a constant CF. For instance, for low-temperature and medium-temperature SHIP with a heat sink thermal capacity of 10 MW$_{th}$, the optimal TES capacity is 12 hours and SM of 2, achieving a CF of 46% and the lowest LCOH of 3.6 ¢/kWh$_{th}$. For high-temperature SHIP, optimal values are a TES capacity of 12 hours and SM of 2.5, achieving a CF of 46% and the lowest LCOH of 4.2 ¢/kWh$_{th}$.

Fig. 6 shows LCOH–CF trends for three cases. In these cases, LCOH exhibits a non-monotonic dependence on CF as the solar field and storage are scaled. At low CF (e.g. with minimal storage and a solar multiple near 1), the system operates only during peak insolation hours, so the capital is underutilized and LCOH is relatively high. Increasing CF by expanding the collector area and adding TES drives LCOH downwards initially, since a greater fraction of the 10 MW$_{th}$ load is met by solar energy, spreading fixed costs over more output. This trend continues until an optimal zone is reached, beyond this point, further CF gains come at the expense of disproportionately larger collector fields and storage units. In other words, the marginal energy yield diminishes as CF approaches the upper limit, so pushing CF too high causes the LCOH to level off and eventually rise again due to escalating capital costs for additional PTC area and storage capacity. This behavior defines an economic trade-off, with a sweet spot at moderate CF where solar utilization is high but the LCOH remains near its minimum.

Differences between temperature cases are evident in the absolute LCOH values and the CF at which this optimum occurs. The lower-temperature systems (Case 1 and 3) consistently achieve lower LCOH at a given CF compared to the high-temperature system, reflecting higher thermal efficiency of PTCs at these operating temperatures. In the 60-250 °C range, the collectors operate near their peak efficiency, yielding a minimum LCOH on the order of 3.6 ¢/kWh$_{th}$ at roughly 45-50% CF. By contrast, the 290-390 °C case suffers greater optical and thermal losses and requires a larger solar field to attain the same CF, resulting in a higher optimal LCOH of about 4.2 ¢/kWh$_{th}$ (achieved at a similar ~46% CF, but with a solar multiple ≈2.5). These results highlight that process heat at lower temperatures is more cost-effectively supplied by solar, a substantial share of the heat demand (CF ~40-50%) can be met with low LCOH in Case 1-3, leveraging the high efficiency of PTCs in the 100-250 °C range. For high-temperature processes (Case 4), solar heat is still feasible but comes at a higher cost per unit energy. The economic optimum occurs at a slightly lower solar fraction, beyond which LCOH rises sharply. Practically, this implies that for industrial processes requiring moderate temperatures, designers can adopt larger solar multiples and storage to maximize solar contribution with minimal cost penalty. In contrast, for ~350 °C processes, a more cautious approach is warranted – optimizing field size and storage to balance fuel savings against capital cost, or using hybrid configurations – to ensure the delivered solar heat remains cost-effective.

To ensure the robustness of these findings, a sensitivity analysis was conducted on critical parameters. Fig. 7

shows tornado diagrams for the sensitivity of the LCOH to the same ±10% parameter variations. The LCOH integrates both the energy output and the cost side, so the sensitivities reflect how design changes affect overall economics.

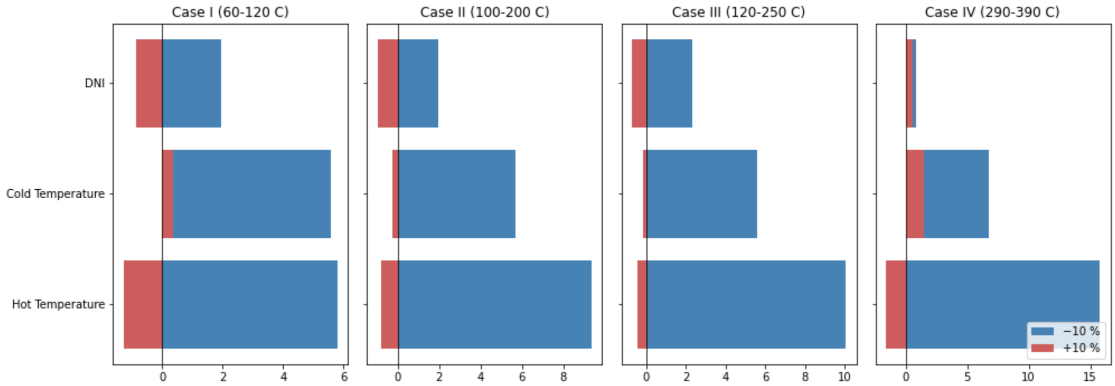

Figure 7: Tornado sensitivity analysis of levelized cost of heat (LCOH) for the four cases. Bars indicate the change in LCOH (¢/kWh$_{th}$) resulting from ±10% changes in the design DNI, HTF outlet temperature, and HTF inlet temperature (baseline LCOH for each case is ~3.5¢ for low-temp, 3.6¢ for mid-temps, and 4.2¢ for high-temp)

Among the parameters considered, the HTF outlet temperature has the strongest effect on LCOH. In all cases, increasing it by 10% reduced LCOH, while lowering it increased cost, with the strongest effect in the high-temperature case. A higher outlet temperature carries more thermal energy per unit mass flow and can improve the use of thermal storage. Design DNI was the second most influential factor: a 10% increase slightly lowered LCOH by reducing the required collector area, whereas a 10% decrease raised it because of field over-sizing. By contrast, the HTF inlet temperature had only a minor and case-dependent effect, typically changing LCOH by about 1-2%. Overall, the results show that accurate DNI estimation is especially important for economic performance. The sensitivity of capacity factor followed the same trend as annual energy output, and Fig. 8 presents the tornado charts for CF in the four cases.

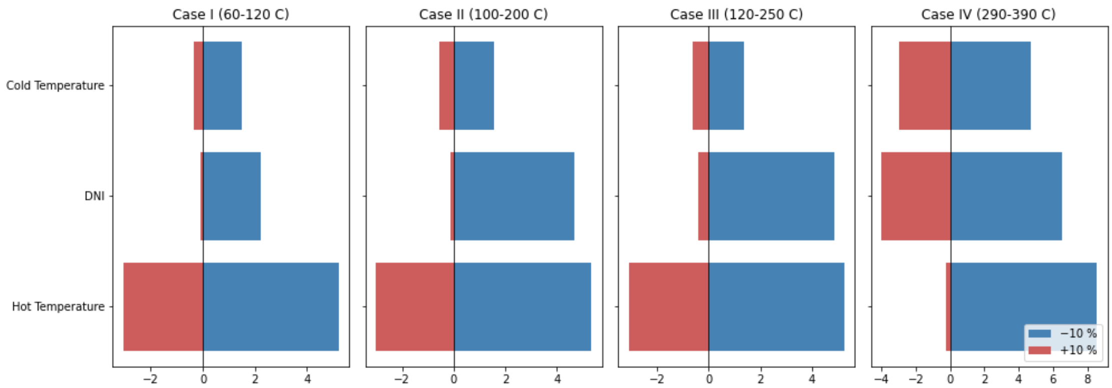

Figure 8: Tornado sensitivity analysis of capacity factor (CF) for the four cases. Bars show the change in annual CF (percentage points) for ±10% variations in design DNI, HTF outlet temperature, and HTF inlet temperature (baseline CF 45–46%).

A 10% decrease in the design DNI (i.e. building a larger field than standard) raises the capacity factor by several percentage points (since the plant is able to collect more energy over the year), whereas a 10% increase in DNI lowers the CF accordingly. In our results, CF changes of roughly ±3-4 points accompanied ±10% DNI changes (e.g. from ~46% down to ~42% or up to ~50%). Variations in the HTF outlet temperature also shift the CF slightly: higher outlet temperatures lead to a small reduction in CF (on the order of 1-2 percentage points in Case 4, and <1 point in Cases 1-3) due to the reduction in yearly output. Lowering the outlet temperature marginally increases CF. The inlet temperature has a negligible effect on CF in low and medium cases (<0.5 point change), and only about ±1 point in the high case for ±10% change. These results reinforce that the solar resource is the dominant factor governing how much of the time the plant can run at full capacity. They also imply that, for planning purposes, modest uncertainties in the HTF temperature requirements will not drastically affect the anticipated solar fraction of heat supply – the system is fairly robust to those assumptions. On the other hand, getting the DNI estimate right is crucial for projecting plant utilization and refining the economic feasibility.

In summary, the sensitivity analysis indicates that our optimized PTC systems maintain competitive performance over reasonable ranges of key parameters. Even in worst-case sensitivity scenarios (e.g. actual DNI 10% lower than expected), the LCOH remained below ~4.5 ¢/kWh_{th} for all cases and the capacity factors stayed above ~40%. This suggests a degree of robustness in the techno-economic viability of solar process heat under Tashkent conditions.

In this section, we compare the cost indicators of optimized SHIP systems, featuring a 10 MW_{th} heat sink and modeled for the selected location in Tashkent, with operational SHIP projects worldwide. Fig. 9, adapted from Energising Europe (2022), shows the LCOH in ¢/kWh_{th} for various energy sources and applications, using data from Eurostat, the Trinomics report prepared for the European Commission, IEA-SHC Task 52 on classification and benchmarking, *Solar Heat Worldwide 2018*, and the Energy Visualisation Portal (europa.eu). This figure also includes the LCOH values for the modeled SHIP across all cases. As shown in Fig. 9, the LCOH for the modeled SHIP plants is lower than the threshold LCOH values established for European countries.

One of the key advantages of using PTCs for SHIP is the potential to significantly reduce greenhouse gas (GHG) and air pollutant emissions. In Uzbekistan, natural gas remains the dominant fuel for industrial heat generation, considered cleaner than coal and oil. However, its combustion still results in substantial carbon dioxide (CO_2) emissions, along with harmful pollutants such as particulate matter (PM), nitrogen oxides (NO_x), and sulfur dioxide (SO_2). Although solar thermal systems may result in minor lifecycle emissions during installation or maintenance, this study assumes zero operational emissions for PTC-based SHIP, focusing on the replacement of combustion-based heating.

To quantify the emission reduction potential, annual CO_2 emissions from natural gas combustion were estimated using the following equation, based on Mohammadi et al. (2021):

$$\text{Annual } CO_2 \text{ emission} = \frac{44.010}{12.011} \times \dot{Q}_{th} \times \frac{CC}{LHV \times \eta_{Boil}} \quad (1)$$

where $\dot{Q}_{th}$ – annual net thermal energy demand (kWh), *CC* – carbon content in the fuel (natural gas) (0.75 kg C/kg fuel), *LHV* – lower heating value of the fuel (13 889 *kWh/kg fuel*) and η_{Boil} – efficiency of a boiler operating on natural gas (0.85). The term 44010/12011 refers to the stoichiometric ratio for the complete oxidation of carbon.

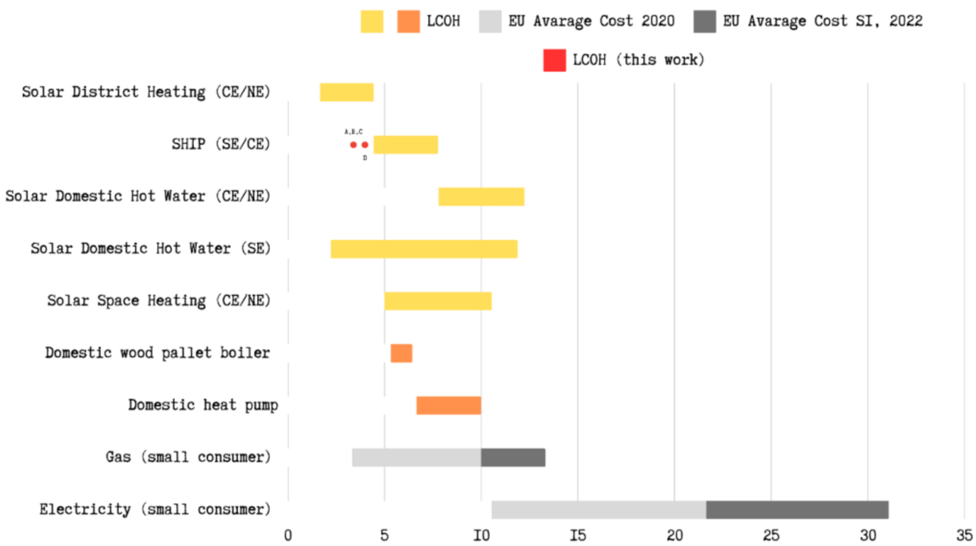

Figure 9: LCOH (¢/kWh_{th}) for various energy sources, adapted from Energising Europe (2022). CE – Central Europe; NE – Northern Europe; SE – Southern Europe; EU – European Union. Red dots indicate the LCOH values for the optimal system cases considered in this work 1, 2, 3 and 4.

This yields a CO_2 emission factor of 0.2328 kg CO_2/kWh_{th}. The same methodology was extended to estimate emissions of PM, NO_x, and SO_2 using corresponding emission factors (Tab. 2), scaled by the annual thermal output.

In parallel, external costs associated with pollutant exposure – including health care burdens, lost productivity, and ecosystem degradation – were assessed. These costs, often excluded from conventional techno-economic evaluations, are included here to capture the broader societal impact of fossil-based thermal energy. Table 2 presents unit damage costs per pollutant, enabling an estimate of the avoided externalities achieved by replacing Natural Gas with solar thermal systems.

Table 2: Emission factors for various pollutants from natural gas combustion, based on the U.S. Environmental Protection Agency (1993).

Pollutants	kg/kWh_{th}
PM	9.616E-06
NO_x	0.00021714
SO_2	9.3058E-07

To contextualize these findings within the urban emissions landscape, data from Tashkent indicate that the transport sector is the largest annual source of CO_2, contributing nearly 50% of citywide emissions. Industry follows with slightly over 40%, while space heating – largely reliant on coal and natural gas – is the third-largest source. However, this ranking contrasts sharply with the $PM_{2.5}$ emission profile reported by the World Bank (2024), in which heating is the dominant source, followed by transport and industry.

The use of PTC-based SHIP offers a dual advantage in this context. By displacing fossil fuels, it simultaneously mitigates CO_2 emissions and reduces local air pollutants, thus generating co-benefits for both climate and public health. Importantly, these benefits accrue during the winter months, when heating demand and pollution levels are at their peak – maximizing the environmental effectiveness of solar thermal integration.

4. Conclusion

This study provides a comprehensive techno-economic and environmental assessment of PTC systems for SHIP under the climatic conditions of Tashkent. Using detailed simulations in the SAM, four representative temperature ranges (60-120 °C, 100-200 °C, 120-250 °C, and 290-390 °C) were analyzed by varying SM = 1-3 and TES = 0-15 h, allowing identification of economically optimal system configurations.

The results demonstrate that system performance and economics are strongly governed by the combined effect of SM and TES, which directly determines the achievable CF and LCOH. Increasing CF initially leads to a pronounced reduction in LCOH due to improved utilization of the solar field and storage assets. However, beyond an optimal range, further CF increases result in diminishing returns and higher LCOH because of rapidly rising capital costs. For low- and medium-temperature applications, the optimal design is achieved at CF ≈ 46% with SM ≈ 2 and TES ≈ 12 h, yielding an LCOH of about 3.6 ¢/kWh_{th}. High-temperature systems require larger solar fields (SM ≈ 2.5) to reach a similar CF, resulting in a higher optimal LCOH of approximately 4.2 ¢/kWh_{th}. These trends confirm that solar heat becomes progressively more expensive at higher process temperatures due to increased thermal and optical losses.

The minimum attainable LCOH occurs at moderate CF values (≈ 35-40%), where low- and mid-temperature systems reach 3.4-3.6 ¢/kWh_{th} with SM ≈ 1.5 and TES ≈ 8 h, while high-temperature systems achieve about 3.8 ¢/kWh_{th} under similar conditions. These values are significantly below reported European benchmark costs, confirming the strong economic competitiveness of PTC-based SHIP in Uzbekistan. In addition, replacing fossil-fuel-based heat with solar thermal systems enables substantial reductions in CO_2, NO_x, SO_2, and particulate matter emissions, directly supporting Uzbekistan's commitments to reduce greenhouse gas emissions by at least 35% by 2030 and to improve urban air quality.

The use of commercially available PTC components (FLABEG RP6 collectors, Schott PTR80 receivers, and Therminol VP-1) ensures reliable operation across a wide temperature range and confirms the technical feasibility of large-scale deployment under Tashkent's moderate solar resource (annual DNI ≈ 1653 kWh/m²). Sensitivity analysis further highlights that accurate assessment of local DNI and proper selection of HTF temperature levels are critical for minimizing economic risk.

5. Acknowledgments

The authors are grateful to NREL for providing access to SAM software. This work was conducted under the budget theme "Development of fundamental principles for the efficient utilization of solar thermal applications with nanofluids and heat storages based on phase change materials" of the Physical-Technical Institute of Uzbekistan Academy of Sciences. The authors also would like to thank the Grant PRIM 01-22 funded by the MUNIS project, which is jointly implemented by the World Bank and the Ministry of Higher Education, Science, and Innovations of the Republic of Uzbekistan.

6. References

Akello, P.O.O., Saoke, C.O., Kamau, J.N., Ndeda, J.O.H., 2023. Modeling and performance analysis of solar parabolic trough collectors for hybrid process heat application in Kenya's tea industry using system advisor model. Sustainable Energy res. 10, 7. https://doi.org/10.1186/s40807-023-00077-w

Aly, A., Bernardos, A., Fernandez-Peruchena, C.M., Jensen, S.S., Pedersen, A.B., 2019. Is Concentrated Solar Power (CSP) a feasible option for Sub-Saharan Africa?: Investigating the techno-economic feasibility of CSP in Tanzania. Renewable Energy, 135, 1224–1240. https://doi.org/10.1016/j.renene.2018.09.065

Avezova N.R., Rakhimov, E.Yu., Khaitmukhamedov A.E., Boliev B.B., Usmanov, A.Yu., 2018. Dependence of Techno-Economic and Ecological Indicators of Flat-Plate Solar Water Heating Collectors in Hot Water Supply Systems from the Temperature of Heating Water. Applied Solar Energy, Vol. 54, Issue 4, pp. 297-301. https://doi.org/10.3103/S0003701X18040035

Dersch, J., Dieckmann, S., Hennecke, K., Pitz-Paal, R., Taylor, M., Ralon, P., 2020. LCOE reduction potential of parabolic trough and solar tower technology in G20 countries until 2030. AIP Conf. Proc. 11 December 2020; 2303 (1): 120002. https://doi.org/10.1063/5.0028883

El Ydrissi, M., H. Ghennioui, E.G. Bennouna, A. Farid, 2020. Techno-economic study of the impact of mirror slope errors on the overall optical and thermal efficiencies-case study: solar parabolic trough concentrator evaluation under semi-arid climate, Renew. Energy 161, 293–308. https://doi.org/10.1016/j.renene.2020.07.015

Energising Europe with Solar Heat | A Solar Thermal Roadmap for Europe, 2022. https://solarthermalworld.org/wp-content/uploads/2022/06/Solar-Thermal-Roadmap-2030.pdf (accessed March 16, 2026)

Glatzmaier, G., 2011. Developing a cost model and methodology to estimate capital costs for thermal energy storage (No. NREL/TP-5500-53066). National Renewable Energy Lab. (NREL), Golden, CO (United States). https://docs.nrel.gov/docs/fy12osti/53066.pdf (accessed March 16, 2026)

IEA. Renewables 2021: Analysis and forecast to 2026. https://www.iea.org/reports/renewables-2021 (accessed March 16, 2026)

Jain, A., Chalapathi Rao, P. N. B. V., Choudhury, P., Mehta, R., & Mittal, S. K., 2013. Optimization studies for hybrid and storage designs for parabolic solar trough systems with the system advisor model. Environmental Progress & Sustainable Energy, 32(4), 1247–1254. https://doi.org/10.1002/ep.11719

Jalilov, D.Y., Juraev, T.I., Akhatov, J.S., 2024. Investigation of the Sedimentation Process in MWCNT-Based Nanofluids with an Influence of Surfactant, Applied Solar Energy, Vol. 60, Issue 2, pp. 281-286. https://doi.org/10.3103/S0003701X23602077

Kasra Mohammadi, Saber Khanmohammadi, Jake Immonen, Kody Powell, 2021. Techno-economic analysis and environmental benefits of solar industrial process heating based on parabolic trough collectors. Sustainable Energy Technologies and Assessments 47, 101412. https://doi.org/10.1016/j.seta.2021.101412

Kumar, L., Hasanuzzaman, M., Rahim, N.A., 2019. Global advancement of solar thermal energy technologies for industrial process heat and its future prospects: a review, Energy Convers. Manag., 195, p. 885–908. https://doi.org/10.1016/j.enconman.2019.05.081

Lovegrove, K., & Stein, W., 2020. Concentrating solar power technology principles – developments and applications book (1st ed.). Woodhead Publishing Limited (accessed March 16, 2026)

Manikandan GK, Iniyan S, Goic R., 2019. Enhancing the optical and thermal efficiency of a parabolic trough collector – A review. Applied Energy, 235, 1524–40. https://doi.org/10.1016/j.apenergy.2018.11.048

Montes, M. J., Abánades, A., Martínez-Val, J. M., & Valdés, M. Solar multiple optimization for a solar-only thermal power plant, using oil as heat transfer fluid in the parabolic trough collectors. Solar Energy, 83(12), 2165–2176 (2009). https://doi.org/10.1016/j.solener.2009.08.010

Mukeshimana, M. C., Zhao, Z.-Y., & Nshimiyimana, J. P., 2021. Techno-economic analysis and viability assessment of concentrating solar power under climatic conditions of Rwanda. International Journal of Energy and Water Resources, 1-17. https://doi.org/10.1007/s42108-021-00161-1

National Renewable Energy Laboratory (NREL), 2023. System Advisor Model (SAM) Software User Guide. https://sam.nrel.gov/images/web_page_files/sam-help-2023-12-17.pdf (accessed March 16, 2026)

REN21. 2023. Renewables 2023 Global Status Report collection, Renewables in Energy Supply. (Paris: REN21 Secretariat) (accessed March 16, 2026)

Resolution of the Cabinet of Ministers of the Republic of Uzbekistan, dated April 16, 2024, No. 204. https://lex.uz/ru/docs/6884060 (accessed March 16, 2026)

Shirmohammadi, R., Aslani, A., Ghasempour, R., Romeo, L. M., & Petrakopoulou, F., 2021. Techno-economic assessment and optimization of a solar-assisted industrial post-combustion CO_2 capture and utilization plant. Energy Reports, 7, 7390–7404. https://doi.org/10.1016/j.egyr.2021.10.091

Steinfeld, A., Wirz, M., and Roesle, M., 2014. Design point for predicting year-round performance of solar parabolic trough concentrator systems. J. Sol. Energy Eng., 136(2): 021019 (7 pages). https://doi.org/10.1115/1.4025709

Tax Committee of the Republic of Uzbekistan, 2026. Retrieved March 16, 2026, from Tax Committee. https://gov.uz/en/soliq (accessed March 16, 2026)

The Central Bank of the Republic of Uzbekistan (CBU), 2026. Retrieved March 16, 2026, from CBU Annual Inflation; CBU Refinancing Rate. https://cbu.uz/en/ (accessed March 16, 2026)

U. S. Environmental Protection Agency, Office of Air Quality Planning and Standards, 1993. EMISSION FACTOR DOCUMENTATION FOR AP-42 SECTION 1.5 LIQUEFIED PETROLEUM GAS COMBUSTION. https://www.epa.gov/sites/default/files/2020-09/documents/emission_factor_documentation_for_ap42_section_1.5_liquified_petroleum_gas.pdf (accessed March 16, 2026)

Wang, Z., 2019. General design of a solar thermal power plant. In Z. Wang (Ed.), Design of solar thermal power plants (pp. 117–224). Academic Press. https://doi.org/10.1016/C2017-0-03007-0

World Bank. 2024. Air Quality Assessment in Tashkent and the Roadmap for Air Quality Management Improvement in Uzbekistan. © World Bank. https://documents1.worldbank.org/curated/en/099061424075531584/pdf/P1771081ec9e93071181d3140144918d6cd.pdf (accessed March 16, 2026)

Wu CH, Wang HC, Chang HY., 2022. Dual-axis solar tracker with satellite compass and inclinometer for automatic positioning and tracking. Energy Sustain Dev, 66, 308–18. https://doi.org/10.1016/j.esd.2021.12.013

Weiss, W., Spork-Dür, M. Solar Heat Worldwide 2024, Institute of Sustainable Technologies AEE, Austria, 2024. https://www.iea-shc.org/Data/Sites/1/publications/Solar-Heat-Worldwide-2024.pdf (accessed March 16, 2026)